Anti-Skid Control for EV Using Dynamic Model Error based on Back-EMF Observer

Lianbing Li, Shinya Kodama, and Yoichi Hori, Senior Member, IEEE

Department of Electrical Engineering, University of Tokyo, 4-6-1 Komaba, Meguro, Tokyo, 153-8505
Email: lilianbing@horilab.iis.u-tokyo.ac.jp, kodama@horilab.iis.u-tokyo.ac.jp,
hori@iis.u-tokyo.ac.jp

***Abstract*— In this paper, a novel anti-skid controller for EV without speed sensor is proposed to prevent the slip between tire and road. Based on back-EMF observer and dynamic model error observer, an anti-skid controller with PI regulator is designed and analyzed. When skid occurs, the equivalent inertia of the EV system will change, and the acceleration of the wheels will also change. A back EMF observer is constructed to acquire the information of speed as well as the acceleration. Then a dynamic model error observer is setup using the signal of back EMF to regulate the torque (current) command, and keep the status of EV within a safe area. By selecting the gains of proportional item and integral item of the regulator, the torque (current) reduction can be adjusted freely in some range, and it is proved that the controller with integral item has better performance in skid restraining. The experimental results of the vehicle simulator utilizing Motor-Generator system verified the effectiveness of our proposed method.**

I. Introduction

Recently a lot of electric vehicles (EV), such as pure electric vehicles, fuel cell vehicles and hybrid vehicles, have been developed to solve the air pollution problems in cities caused by the traditional internal combustion engine vehicles (ICV). With the driving of electric motor, the vehicles can also achieve high-performance dynamic control ability[1]. In the motion process of a vehicle, the adhesion characteristics between tire and road surface have great effect on the motion status of the vehicle. This means that in order to improve the stability and safety of vehicle, it is necessary to adjust the driving and braking torque of the system to control the adhesion status of each wheel. At the same time, if the adhesion status can be controlled effectively, the energy loss will be cut down, and the distance of one battery charge will be also expanded.

In order to acquire better adhesion performance for any type of road conditions, the skid prevention controller should to be designed. The slip caused by accelerating, decelerating or braking usually leads to unsafe motion in vehicle driving. Motion stabilization[2] and lateral motion control[3] can keep the motion status within a safe area. As the base of the vehicle motion stabilization, the skid preventing technologies are developed, such as Model Following Control (MFC)[1], [4], optimal slip ratio control[5]. Current disturbance observer also be used to limit the fast increasing of the wheel speed[6]. The anti-skid controllers based on disturbance observer[7] or road conditions estimator[5], [8] are also studied recently. In most of these control schemes, the wheel speed even the vehicle speed is needed. In this paper, a novel back-EMF based anti-skid controller algorithm is proposed. Based on the characteristic of the back EMF, a dynamic model error observer is set up. It can follow the input command of current, and when slip occurs, the output torque will be decreased quickly to prevent increasing slip.

II. Analysis of Tire-Road System

The problem of wheel slip control can be analyzed by using a one-wheel-car model[9] as shown in Fig. 1. There are two inertias in this system, the rotating wheel and the body of the car. The dynamic equation of the system can be expressed as

$$\dot{\omega} = \frac{T - F_d r - F_w(\omega) r}{J_w} \tag{1}$$

$$\dot{V} = \frac{F_d - F_V(V)}{M} \tag{2}$$

where T is the sum of driving and braking torques, i.e. T=$T_d - T_b$; F_d is the drive force of the chassis, F_w is the average friction force of the driving wheels for acceleration and the average friction force of all wheels for deceleration, J_ω is the inertia of the wheels, F_V is the wind force of the vehicle. M is the mass of the chassis and the wheels of the vehicle, i.e. $M = M_v + M_w$.

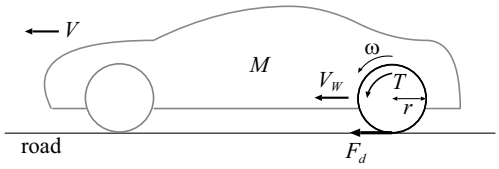

Fig. 1. One-wheel vehicle model.

The slip ratio λ is used to describe the slip status between the road and the tire. It is defined as

$$\lambda = \frac{V_W - V}{V_W} \quad \text{(Driving)} \tag{3}$$

$$\lambda = -\frac{V - V_W}{V} \quad \text{(Braking)} \tag{4}$$

where V_W is the wheel speed, V is the velocity of the chassis.

The friction coefficient μ is a function of of slip ratio λ, $\mu = f(\lambda)$, which is dependent on the road conditions. For different conditions of the road such as dry, wet, snowy, etc., the relationship between λ and μ is different.

The drive force of the vehicle F_d is proportional with the friction coefficient and the pressure to road. After having

achieved the friction coefficient μ from slip ratio λ utilizing $\mu - \lambda$ curve, the driving force F_d can be calculated by

$$F_d = N\mu(\lambda) \tag{5}$$

where N is the normal component of reactive effect on tires. The block diagram of the vehicle is shown in Fig.2.

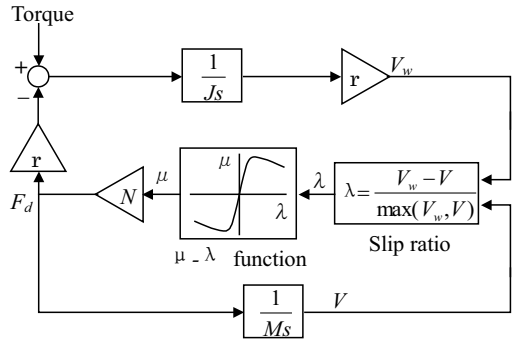

Fig. 2. The block diagram of the vehicle.

III. The Anti-Skid Scheme Utilizing Dynamic Model Error Observer

A. Back-EMF Observer

In the condition of no speed sensor, the anti-skid controller can also be realized with other signals such as back EMF. This kind of slip controller has more reliability and more robust performance. But the signal of back EMF cannot be detected directly, it is necessary to set up an observer to estimate the value of back EMF. A current disturbance observer with variable gain and time constant is discussed in paper [6], which utilized the torque drop characteristic to limit the torque when slip occurs. The current disturbance observer is used to compensate the voltage drop caused by back EMF, so in fact it is also a back EMF observer. In this paper it is employed to estimate the back EMF, as shown in Fig.3.

The estimated back EMF can be expressed as

$$\hat{V}_{emf} = \frac{u^* - (Ls + R)i}{\tau s + 1} \tag{6}$$

where the $\frac{1}{\tau s+1}$ is a low-pass filter for restraining the noise of the estimated value. In the inner loop of the controller, an

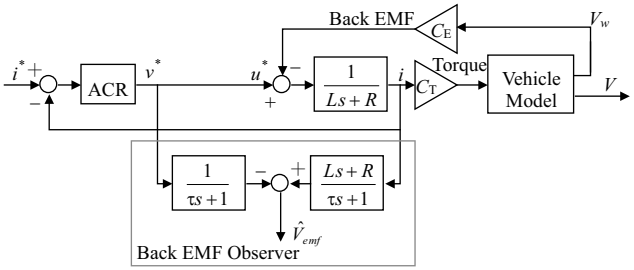

Fig. 3. The block diagram of back-EMF observer.

appropriate current regulator (ACR) is designed to follow the current command quickly.

B. The Anti-Skid controller based on Dynamic Model Error Observer

It is well known that the value of back EMF is proportional with the motor speed, (6) can be written as

$$\hat{V}_{emf} = \omega C_e \frac{1}{\tau s + 1} \tag{7}$$

The model of vehicle will change when skid occurs. So it is possible to construct a dynamic model error observer using the estimated back-EMF signal, i.e. wheel speed signal, as shown in Fig.5.

$$\varepsilon_m = V_{emf} * (J/C^2)s - i^* \tag{8}$$

By this approach, the system model disturbance can be observed without speed sensor. In Fig.5, as the current is proportional with the torque, the load torque can be expressed by its current i_L, and i_d is the motivate current of F_d.

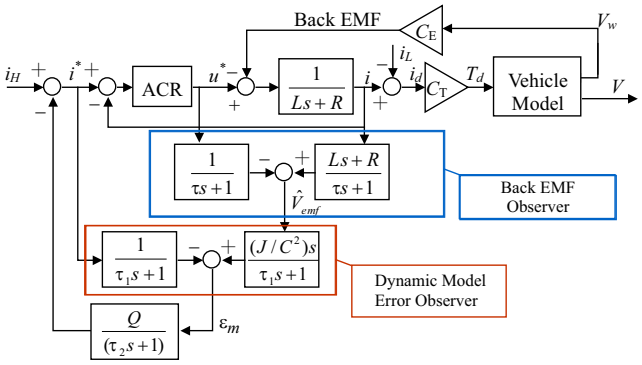

Fig. 4. Slip prevention system based on load disturbance observer.

As the time constant of the inner loop is more than 10 times as small as that of the outer loop, in order to simplify the dynamic analysis of the system, the transfer function from i^* to i is considered as 1. Thus the open loop transfer function from human drive command i_H to the drive current i_d is

$$G_{OL} = \frac{Q}{(\tau_1 s + 1)(\tau_2 s + 1) - Q} \tag{9}$$

If $Q = K_p, (K_p \in \mathbf{R})$, then the Bode diagram of the open transfer function can be drawn as shown in Fig.5. The Bode diagram shows that, when $K_p <= 1$, the gain margin and phase margin are big enough, but when $K_p > 1$, due to the small stability margin, the system will have poor robust performance against uncertainty in low and high frequency parts.

The closed loop transfer function from i_H to i_d is

$$G_{CL} = \frac{(\tau_1 s + 1)(\tau_2 s + 1)}{(\tau_1 s + 1)(\tau_2 s + 1) + K_p(J_n/J - 1)} \tag{10}$$

It indicates that, when $J = J_n$, the closed loop transfer function will be equal to 1. That is, the current command, i.e. current (torque) command will be exactly realized by the controller. And if slip happens, the inertia J will decrease, and the transfer function will also decrease with the change of J. On the other hand, when J increases, the transfer function will also increase to keep the acceleration as a constant value.

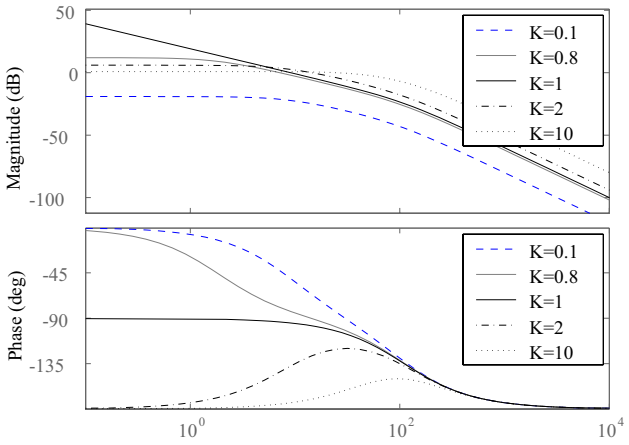

Fig. 5. Slip prevention system based on load disturbance observer.

C. Slip controller with Integral Regulator

In order to insure the robust performance of the slip controller, it's better to limit the gain of the controller within 1. However, in most of the slip situations, the wheel acceleration should be decreased in some extend to prevent more slip. It requires that the gain is big than 1.

In the slip process, the difference between feed forward and feedback of the dynamic model error observer is various with the different slip status. And if the slip is serious, the model error is also big. So an integrator is tried to put into the controller, i.e. $Q = K_p + K_i/s, (K_p, K_i \in \mathbf{R})$, to regulate the torque dropping command.

The open loop transfer function from human drive command i_H to the drive current i_d becomes

$$G_{OL} = \frac{K_p s + K_i}{s(\tau_1 s + 1)(\tau_2 s + 1) - K_p s - K_i} \tag{11}$$

The bode diagram of the system with different K_i and $K_p = 1$ is shown in Fig.6.

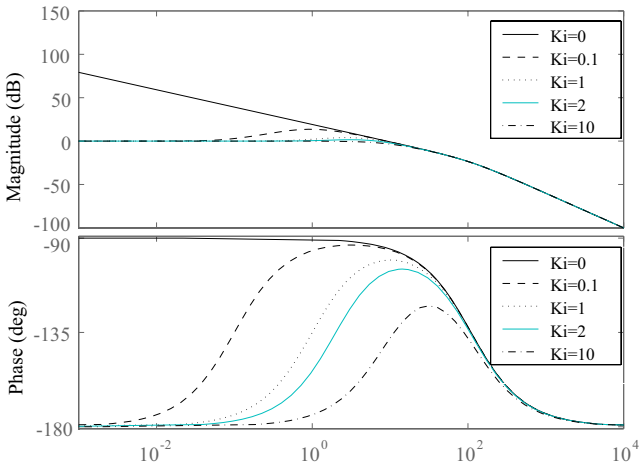

Fig. 6. Bode diagram of the system with integral regulator.

The closed loop transfer function from i_H to i_d becomes

$$G_{CL} = \frac{(\tau_1 s + 1)(\tau_2 s + 1)s}{s(\tau_1 s + 1)(\tau_2 s + 1) + (K_P s - K_I)(J_n/J - 1)} \tag{12}$$

It indicates that, when $J = J_n$, the closed loop transfer function will also be equal to 1, that is, the current command, i.e. current (torque) command will be exactly realized by the controller. And if the slip happens, the J will decrease, and the transfer function will also decrease with the change of J.

The comparison of the controllers with different parameters is shown in Fig.7. From to the bode diagram, it is found that the phase curve that the integral gain K_i is 10 is similar with the one of $K_p = 2$.

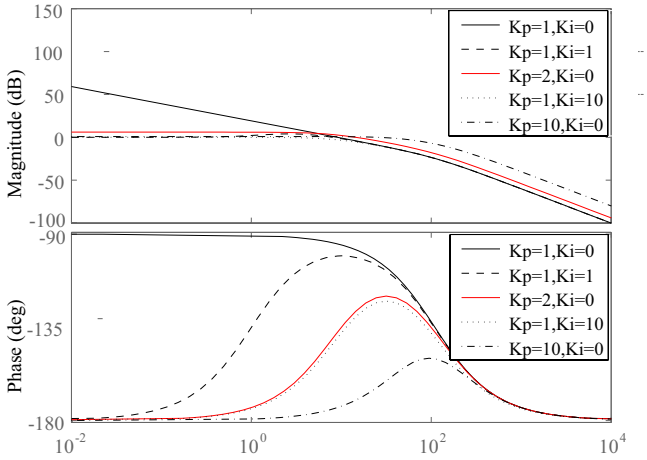

Fig. 7. Comparison of the controllers with different parameters.

Of course, the integral part of the regulator is need to cut off when the adhesion recovered.

IV. Simulation and Experiment Results

Suppose that the vehicle is running from the dry road to the icy road, and the surface of the icy road is very smooth, so that the friction between the tire and the road rapidly reduces. At the same time, if the motor of the EV is still keeping the driving torque as before, then the wheel will slip on the icy road quickly. The slip phenomenon is simulated by MATLAB utilizing the EV system as shown in Fig.2 and Fig. 4. Suppose the EV starts to accelerate on the dry road from $t = 0$sec, and at $t = 3$sec it enters the icy road. The parameters of the EV system are used with the ones of "UOT March I" which is the experimental EV of our laboratory. In order to compare with the experiment, the simulation outputs are proportionally converted into the scope of the experiment results.

A. Simulation Results

In order to find the relationship between the performance of the slip controller and the gain of the load torque observer K_p and K_i, the controllers with parameters of different K_p and different K_i are simulated and the simulation results are shown in Fig.8 and Fig.9, respectively. In Fig.8, the gain of the load torque observer K_p, the gain is changed from 0.1 to 10. When $K_p = 0$, as shown in Fig.8 (a) and (c), the wheel speed dramatically increases after slip occurred.

When $K_p = 1$, the acceleration always keep the constant value, the fast increase of the speed is limited. When $K_p > 1$, the wheel speed is decreased after slip happened. The torque and the output of the observer shown in Fig.8(b) also proved this point. So the slip ratio is limited as the K_p increases as shown in Fig.8(d).

In Fig.9, with the conditions of $K_p = 1, K_i = 0 \cdots 10$, the results prove that with the increase of K_i, the drop of the acceleration become large and the slip ratio is restrained effectively.

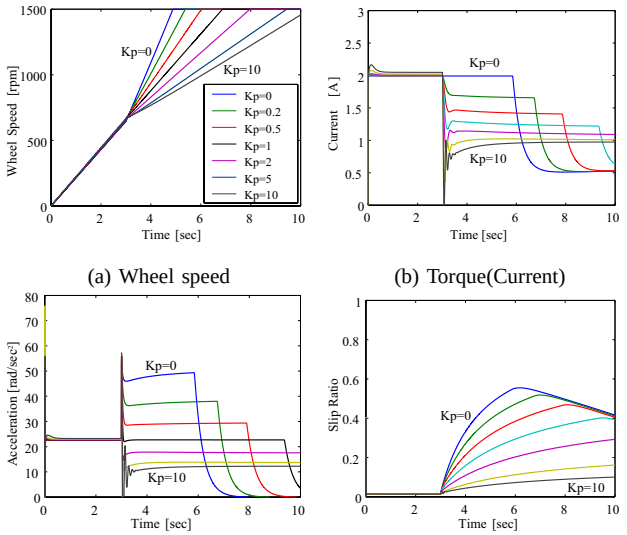

(a) Wheel speed (b) Torque(Current)

(c) Acceleration (d) Slip ratio.

Fig. 8. Simulation results with $K_p = 1, K_i = 0 \cdots 10$

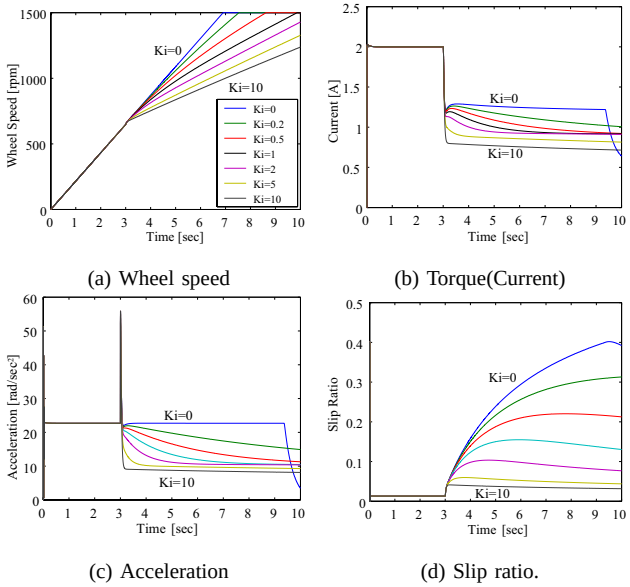

(a) Wheel speed (b) Torque(Current)

(c) Acceleration (d) Slip ratio.

Fig. 9. Simulation results of EV

For comparing the two sets of curves, the comparison curves with the parameters of $[K_p = 2, K_i = 0], [K_p = 1, K_i = 1]$ and $[K_p = 10, K_i = 0], [K_p = 1, K_i = 10]$ are shown in Fig.14 (a) and (b). In Fig.14, the acceleration drop of $[K_p = 1 K_i = 1]$ is bigger than that of $[K_p = 2 K_i = 0]$ in the whole process. And the controller of $[K_p = 1 K_i = 10]$ has better slip preventing performance than other ones as shown in the Fig.14.

B. *Experiments Results*

In this paper, the DC Motor-Generator system, as shown in Fig.10, is designed to simulate the EV system with slip phenomenon[6]. The block diagram is shown in Fig.11. In the M-G set, the drive motor and the load motor can be controlled dependently. And an inertia simulator is designed to simulate the varying of the equivalent inertia of the EV system.

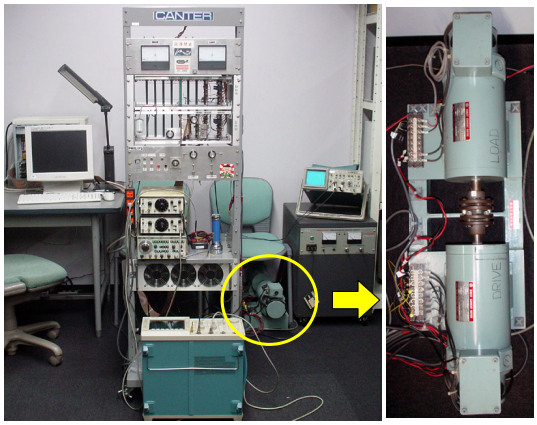

Fig. 10. Experimental system.

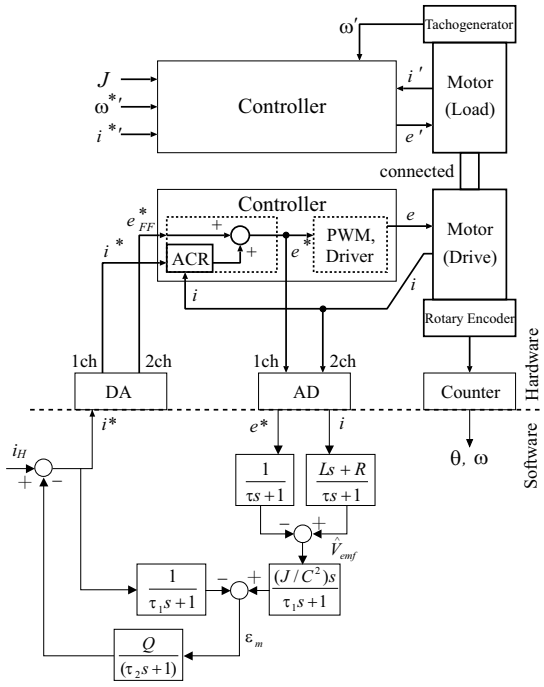

Fig. 11. Block diagram of experimental system.

The experiment results are shown in Fig.12 and Fig.13. The curves have the same features with the ones of simulation results shown in Fig.8 and Fig.9 expect for some noises. With the increase of K_p or K_i, the acceleration, as well as the slip ratio, is limited effectively. And the comparison curves as shown Fig.14 (c) and (d), which indicates that

the adjusting of K_i has more effectiveness than that of K_p.

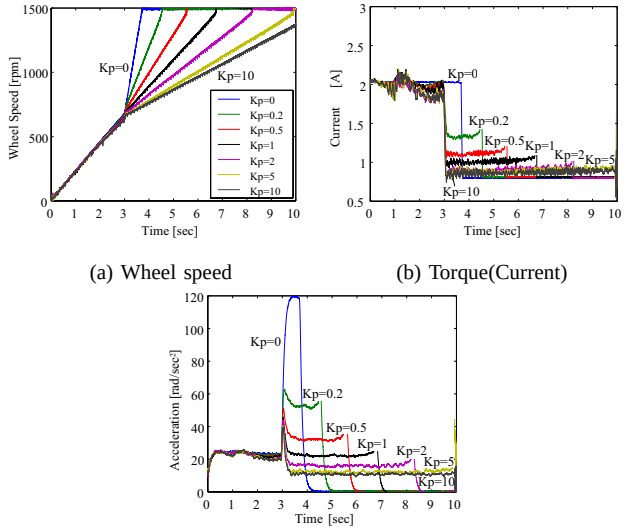

(a) Wheel speed (b) Torque(Current)

(c) Acceleration

Fig. 12. Experiment results of proportional regulator.

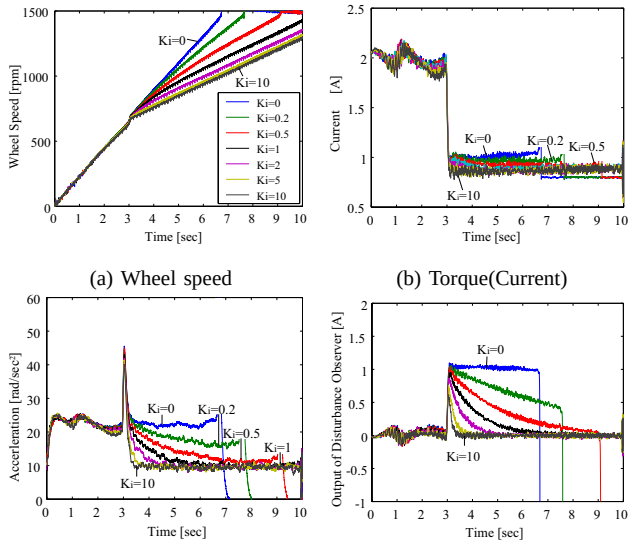

(a) Wheel speed (b) Torque(Current)

(c) Acceleration (d) Dynamic model error ε_m

Fig. 13. Experiment results of regulator with integral part.

V. Conclusion

Using the back-EMF observer and dynamic model error observer, the novel anti-skip controller can be achieved without speed sensor. It can reduce the dependence on the wheel encoder, and enhance the reliability of the system. By analysis of the frequency response, the regulator with integral part also is also proved that it can improves the robust performance of the controller. The simulation and experiment prove that the torque reduction of the speed-sensorless controller can prevent the skid phenomenon effectively, especially in process of accelerating control.

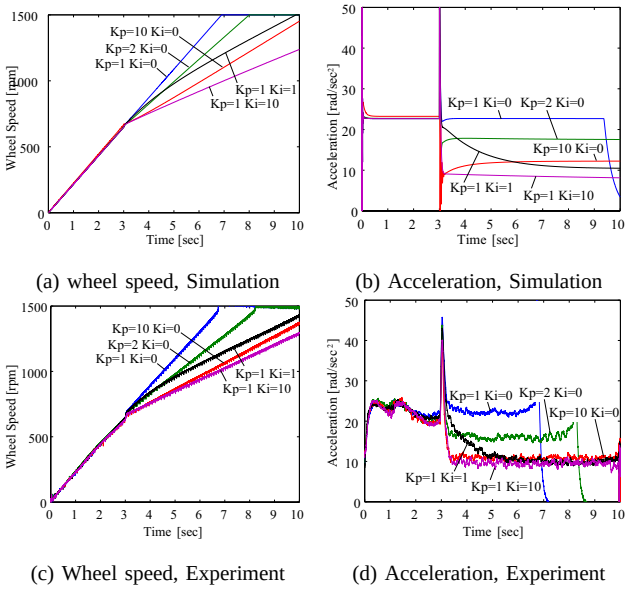

(a) wheel speed, Simulation (b) Acceleration, Simulation

(c) Wheel speed, Experiment (d) Acceleration, Experiment

Fig. 14. Comparison of simulative and experimental results of the controllers with different parameters.

References

[1] Yoichi Hori, Toyoda Y., Tsuruoka, Y. Traction control of electric vehicle: basic experimental results using the test EV "UOT electric march". *IEEE Trans. on Industrial Application*, Vol.34, No.5, 1998, pp.1131-1138.

[2] Hiroshi Fujimoto, Takeo Saito, Toshihiko Noguchi. Motion Stabilization Control of Electric Vehicle under Snowy Conditions Based on Yaw-Moment Observer, *The 8th IEEE International Workshop on Advanced Motion Control*, Kawasaki, March 2004, pp.35-40.

[3] Shin-ichiro Sakai and Yoichi. Hori, Lateral motion stabilization of 4 wheel-motored ev based on wheel skid prevention, *Proc. The 17th. Electric Vehicle Symposium (EVS)*, Montreal, Canada, 2000.

[4] S. Sakai and Y. Hori, Advantage of Electric Motor for Anti Skid Control of Electric Vehicle, *EPE Journal*, Vol.11, No.4, 2001, pp.26-32.

[5] S. H. Kataoka. Optimal Drive Force Control of EV based on Road Status Observing. *Master dissertation of the University of Tokyo*, 2001.

[6] Shinya Kodama, Lianbing Li, Yoichi Hori. Skid Prevention for EVs based on the Emulation of Torque Characteristics of Separately-wound DC Motor, *AMC'04*, Kawasaki, March 2004, pp.75-80.

[7] T. Miyamoto and Y. Hori, Adhesion Control of EV Based on Disturbance Observer, *IEE of Japan Technical Meeting Record*, IIC-00-9, 2000, pp.49-54. [In Japanese]

[8] Shin'ichiro Sakai, Hideo Sado and Yoichi Hori, Dynamic Driving/Braking Force Distribution in Electric Vehicle with Independently Driven Four Wheels. *Electrical Engineering in Japan*, Vol.138, No.1, January 2002, pp.79-89.

[9] Cem Unsal, Pushkin Kachroo. Sliding Mode Measurment Feedback Control for Antilock Braking System. in *IEEE Transactions on Control Systems Technology*, Vol. 7, No. 2, MARCH 1999, pp.271-281.